JACS
JOURNAL OF THE AMERICAN CHEMICAL SOCIETY
Article
pubs.acs.org/JACS

$Li_{14}Ln_5[Si_{11}N_{19}O_5]O_2F_2$ with Ln = Ce, Nd—Representatives of a Family of Potential Lithium Ion Conductors

Saskia Lupart,[†] Giuliano Gregori,[‡] Joachim Maier,[‡] and Wolfgang Schnick[†,*]

[†]Ludwig-Maximilians-Universität, München, Buntenandtstr. 5-13, D-81377 München, Germany
[‡]Max-Planck-Institut für Festkörperforschung, Heisenbergstr. 1, D-70569 Stuttgart, Germany

Supporting Information

ABSTRACT: The isotypic layered oxonitridosilicates $Li_{14}Ln_5[Si_{11}N_{19}O_5]O_2F_2$ (Ln = Ce, Nd) have been synthesized using Li as fluxing agent and crystallize in the orthorhombic space group *Pmmn* (Z = 2, $Li_{14}Ce_5[Si_{11}N_{19}O_5]O_2F_2$: a = 17.178(3), b = 7.6500(15), c = 10.116(2) Å, $R1$ = 0.0409, $wR2$ = 0.0896; $Li_{14}Nd_5[Si_{11}N_{19}O_5]O_2F_2$: a = 17.126(2), b = 7.6155(15), c = 10.123(2) Å, $R1$ = 0.0419, $wR2$ = 0.0929). The silicate layers consist of *dreier* and *sechser* rings interconnected via common corners, yielding an unprecedented silicate substructure. A topostructural analysis indicates possible 1D ion migration pathways between five crystallographic independent Li positions. The specific Li-ionic conductivity and its temperature dependence were determined by impedance spectroscopy as well as DC polarization/depolarization measurements. The ionic conductivity is on the order of 5×10^{-5} S/cm at 300 °C, while the activation energy is 0.69 eV. Further adjustments of the defect chemistry (e.g., through doping) can make these compounds interesting candidates for novel oxonitridosilicate based ion conductors.

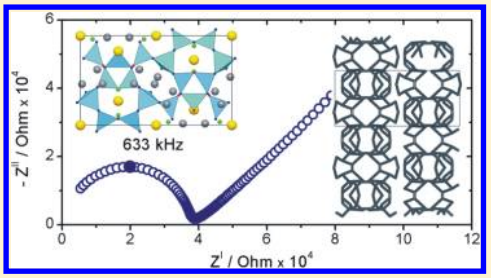

INTRODUCTION

As the need for mobile power supply and efficient energy storage has constantly increased in the last decades, rechargeable batteries have become a key technology in modern society.[1−4] In the effort to meet the demand for effective batteries, lithium based electrochemical devices play a major role; however, most make use of organic liquid electrolytes that require relatively stringent safety precautions and hence are rather inapplicable for a large range of applications (e.g., large-scale systems, medical devices).[1] Nonflammable, nonvolatile solid electrolytes have the potential to overcome these problems, but the assortment of materials that combine all of the basic requirements for all-solid-state batteries, i.e., high ionic conductivity at the operating temperature and a high chemical, electrochemical, and thermal stability, is still restricted.[5,6]

Therefore, great effort has been put into the search for new solid electrolytes and a variety of crystalline, glassy, or composite materials have been considered.[1−3,7] Although Li_3N has one of the highest ionic conductivities at room temperature (6×10^{-3} S cm^{-1}), novel materials are mostly oxides (e.g., $Li_{2+2x}Zn_{1-x}GeO_4$ ($-0.36 < x < 0.87$)[8] or perovskite-related compounds like $La_{0.62}Li_{0.16}TiO3$)[9] or sulfides (e.g., $Li_{3.25}Ge_{0.25}P_{0.75}S_4$[10] or $Li_{10}GeP_2S_{12}$).[5] Only a few rare exceptions, e.g., $Li_xPO_yN_z$ ($x = 2y + 3z - 5$),[11] represent nitrides or oxonitrides. In this context, multinary lithium (oxo)nitridosilicates might be interesting candidates for solid-state electrolytes.

Nitridosilicate based ceramics in general exhibit a high chemical stability combined with high decomposition temperatures and high mechanical strength and are often resistant against oxidation and corrosive environments.[12,13] In addition, the ternary phases $LiSi_2N_3$,[14,15] Li_2SiN_2,[15−17] Li_5SiN_3,[18,19] Li_8SiN_4,[15,17] and $Li_{18}Si_3N_{10}$,[17] reported in the quasi-binary system $Li_3N-Si_3N_4$, all show lithium ion conduction (for example Li_2SiN_2: σ(400 K) = 1×10^{-3} S cm^{-1}; Li_8SiN_4: σ(400 K) = 5×10^{-2} S cm^{-1}).[15,20,21] These facts lead us to expect perceptible Li ion conduction also in multinary lithium (oxo)nitridosilicates.

In recent years, we have structurally elucidated a number of alkaline earth as well as rare earth (oxo)nitridosilicates: e.g., $LiCa_3Si_2N_5$,[22] $Li_4M_3Si_2N_6$ with M = Ca, Sr,[23] $Li_2Sr_4[Si_2N_5]N$,[24] $Li_5Ln_5Si_4N_{12}$ with Ln = La, Ce,[25] $LiLn_5Si_4N_{10}O$ with Ln = La, Pr,[26] and $Li_{35}Ln_9Si_{30}N_{59}O_2F$ with Ln = Ce, Pr.[27] These compounds not only differ in their nominal amount of lithium in their formula units, but also exhibit different silicate substructures covering the whole range of dimensionality, i.e., from isolated groups over layered Si−N substructures up to three-dimensional networks.

In this work, we report about the synthesis and structural characterization of a novel layer-like (oxo)nitridosilicate $Li_{14}Nd_5[Si_{11}N_{19}O_5]O_2F_2$ and its isotypic Ce-containing phase. The complementary electrical conduction measurements prove that these compounds are indeed Li ion conductors with a very large ionic transference number. Yet, further adjustments of the defect chemistry of this material (e.g., through aliovalent cation doping) are required to obtain ionic conductivity values which might be interesting for battery applications.

Received: March 7, 2012
Published: May 1, 2012

   dx.doi.org/10.1021/ja302255d | J. Am. Chem. Soc. 2012, 134, 10132−10137

EXPERIMENTAL SECTION

Synthesis. All manipulations were performed with rigorous exclusion of oxygen and moisture in an argon-filled glovebox (Unilab, MBraun, Garching, O_2 < 0.1 ppm, H_2O < 0.1 ppm). The title compounds can be synthesized using two different routes:

Route 1: One route uses tantalum crucibles (wall thickness 0.5 mm, internal diameter 10 mm, length 300 mm), which were arc-welded under a pressure of 1 bar purified argon. The crucible holder was cooled in order to avoid decomposition reactions during welding. Single crystals of $Li_{14}Ln_5[Si_{11}N_{19}O_5]O_2F_2$ with Ln = Ce, Nd were synthesized from 23.6 mg silicon diimide (0.40 mmol, synthesized according to literature),[28] 25 mg LiN_3 (0.52 mmol, synthesized according to literature),[29] 108.4 mg CeF_3 (0.55 mmol, Sigma Aldrich, 99.9%) for Ln = Ce and 10 mg CeF_3 (0.05 mmol, Sigma Aldrich, 99.9%) as well as 190 mg $NdBr_3$ (0.50 mmol, Sigma Aldrich, 99.9%) for Ln = Nd. A 20-mg portion of Li as fluxing agent were added. After closing, the tantalum crucibles were placed in silica tubes (under argon) which in turn were positioned in the middle of a tube furnace. The temperature was raised to 1000 °C (5 °C/min), maintained for 24 h, subsequently cooled down to 500 °C (0.5 °C/min), and finally quenched to room temperature.

Route 2: To obtain higher amounts of $Li_{14}Ln_5[Si_{11}N_{19}O_5]O_2F_2$ with Ln = Ce, Nd tungsten crucibles heated in a radio frequency furnace under purified nitrogen were used. 63.8 mg silicon diimide (1.10 mmol, synthesized according to literature),[28] 17 mg Li_2O (0.29 mmol, Alfa Aesar, 99.5%) and 98.6 mg CeF_3 (0.50 mmol, Sigma Aldrich, 99.9%) or a mixture of 191.9 mg $NdBr_3$ (0.97 mg, Sigma Aldrich, 99.9%) and 20 mg CeF_3 (0.10 mg, Sigma Aldrich, 99.9%) were mixed in an agate mortar, filled in a tungsten crucible, and covered with 20 mg Li as fluxing agent. The tungsten crucible was placed in a radio frequency furnace and heated within 2 h to 1000 °C. For the Ce-containing compound, the mixture was cooled down over 15 h to 950 °C and subsequently cooled to room temperature within 2 h. The Nd-compound yielded higher purity by maintaining 1000 °C for 15 h, cooling to 800 °C in 1 h, and subsequently quenching the sample to room temperature by switching off the furnace.

Chemical Analysis. Scanning electron microscopy was performed using a JEOL JSM 6500F equipped with a field emission gun at an acceleration voltage of 10 kV with a Si/Li EDX detector (Oxford Instruments, model 7418). Samples were prepared by placing single crystals on adhesive conductive pads and subsequently coating them with a thin conductive carbon film. Each EDX spectrum (Oxford Instruments) was recorded with the analyzed area limited onto the face of one single crystal to avoid the influence of possible contaminating phases. Analysis of three spots per crystallite showed an average atomic ratio Ln: Si = 1: 2.2 which corroborates the composition $Li_{14}Ln_5[Si_{11}N_{19}O_5]O_2F_2$ (Ln = Ce, Nd). For the Nd-containing compound an average of 0.7% Ce content has been found. The determined composition is within the typical error ranges with regard to the fact that lithium cannot be detected by this method and fluorine could not be detected quantitatively, measured values varied between 0−4 atom-% (calcd. (at%):Ln (Ln = Ce, Nd) 9, Si 19, N 33, O 12, F 3; found (at%) Ce 9, Si 20, N 48, O 18; Nd 10, Ce 0.7, Si 22, N 46, O 21).

Single-Crystal X-ray Analysis. Single-crystal X-ray diffraction data were collected with a Stoe IPDS I (Mo-K_α radiation). The program package SHELX97 was used for structure solution and refinement (see Table 1).[30,31]

X-ray Powder Diffraction. X-ray powder diffraction data were collected with a HUBER G670 diffractometer equipped with an imaging-plate system using Cu−$K_{\alpha1}$ radiation (Ge monochromator, λ = 1.54051 Å). For temperature-dependent X-ray powder diffraction, a sample of $Li_{14}Nd_5[Si_{11}N_{19}O_5]O_2F_2$ was enclosed in a silica glass capillary with 0.5-mm diameter under argon atmosphere. The data were obtained with a STOE STADI P diffractometer equipped with an imaging plate system using Mo−$K_{\alpha1}$ radiation (Ge monochromator, λ = 0.71093 Å) in Debye−Scherrer geometry using a graphite furnace. Data were collected every 50 °C starting from room temperature up to 900 °C with a heating rate of 5 °C/min. In this temperature range, the compound undergoes no phase transition or decomposition and therefore it can be assumed that $Li_{14}Nd_5[Si_{11}N_{19}O_5]O_2F_2$ is temperature stable at least until 900 °C.

Table 1. Crystallographic Data of $Li_{14}Ln_5[Si_{11}N_{19}O_5]O_2F_2$ (Ln = Ce, Nd)

	Ln = Ce	Ln = Nd
formula mass/g mol^{-1}	1522.94	1543.54
crystal system	orthorhombic	
space group	*Pmmn* (59)	
cell parameters/ Å	a = 17.178(3)	a = 17.126(2)
	b = 7.6500(15)	b = 7.6155(15)
	c = 10.116(2)	c = 10.123(2)
cell volume/10^6 Å^3	1329.3(5)	1320.3(5)
formula units/cell	2	
$\rho_{calc.}$/g cm^{-3}	3.785	3.883
F(000)	1386	1406
diffractometer	Stoe IPDS I	
temperature/K	293(2)	
radiation, monochromator	Mo−K_α, (λ = 0.71073 Å), graphite	
absorption correction	semiempirical	
θ range/ °	2.3−30.5	
measured reflections	10928	10825
independent reflections	1034	1047
observed reflections	1684	1589
refined parameter	144	
GoF	0.876	0.893
R indices [$F_o^2 \geq 2\sigma(F_o^2)$]	$R1$ = 0.0409, $wR2$ = 0.0896	$R1$ = 0.0419, $wR2$ = 0.0929
R indices (all data)	$R1$ = 0.0699, $wR2$ = 0.0971[a]	$R1$ = 0.0678, $wR2$ = 0.1005[b]
max./min res. electron density/eÅ^{-3}	1.67/ −2.97	2.11/ −2.51

[a] $w = [\sigma^2(F_o^2) + (0.0572P)^2]$, in which $P = (F_o^2 + 2F_c^2)/3$. [b] $w = [\sigma^2(F_o^2) + (0.0574P)^2]$, in which $P = (F_o^2 + 2F_c^2)/3$.

Electrical Conductivity Measurements. For the electrical conductivity measurements, two different sets of samples were prepared: (i) a series of pellets with a diameter of 6 mm and thickness of ∼3.5 mm were obtained by uniaxially cold pressing (350 MPa) the $Li_{14}Ln_5[Si_{11}N_{19}O_5]O_2F_2$ powder; (ii) a symmetric cell consisting of the following five layers (containing electron-blocking elements, LiI) was assembled LiAl/LiI/$Li_{14}Ln_5[Si_{11}N_{19}O_5]O_2F_2$/LiI/LiAl. In this case, the powders were first uniaxially pressed (250 MPa) and subsequently isostatically pressed at 500 MPa for 5 min. The $Li_{14}Ln_5[Si_{11}N_{19}O_5]O_2F_2$ layer had a final diameter of ∼5 mm and thickness of about 0.5 mm.

AC measurements were performed using a Novocontrol high resolution dielectric analyzer at frequencies ranging between 1 MHz and 0.01 Hz (AC voltage of 0.3 V, titanium electrodes). DC measurements were carried out by applying a 10 nA current (galvanostatic mode) with a Keithley 220 current source and measuring the voltage response with a Keithley 6514 system electrometer. The impedance spectra were analyzed using the commercial software Z-View by Scribner Assoc.

RESULTS AND DISCUSSION

Synthesis and Crystal Structure. The air and moisture stable compounds $Li_{14}Ln_5[Si_{11}N_{19}O_5]O_2F_2$ with Ln = Ce, Nd were synthesized using liquid lithium as fluxing agent at temperatures around 1000 °C. The title compounds can be synthesized analogously with two different synthetic approaches (see Experimental Section): In closed ampules (tantalum or niobium) with additional LiN_3 in a tube furnace or in "open" tungsten crucibles in a radio frequency furnace with about 1 bar purified dynamic nitrogen atmosphere. However, the results

dx.doi.org/10.1021/ja302255d | J. Am. Chem. Soc. 2012, 134, 10132−10137

from both synthetic approaches differ slightly from each other: in closed systems (tantalum or niobium ampules), only smaller amounts of the title compounds were accessible and Ta-containing side phases were unavoidable, whereas in tungsten crucibles, it is possible to obtain larger amounts of the samples, although elemental lithium is used in an open reaction system. In the system Ce–Si–O–N, many thermodynamically stable phases exist, which cannot be completely excluded. The Nd phase can only be obtained as single crystals with 0.7 atom-% Ce-content. Due to the reasons listed above, we focused for the physical measurements on the Nd-containing phase, which was synthesized in a radio frequency furnace. To avoid impurities, single crystals of $Li_{14}Nd_5[Si_{11}N_{19}O_5]O_2F_2$ were isolated from the obtained samples for the measurements.

The two isotypic compounds $Li_{14}Ln_5[Si_{11}N_{19}O_5]O_2F_2$ with Ln = Ce, Nd crystallize in the orthorhombic space group *Pmmn* with two formula units per cell (for details see Table 1). Oxygen has been assigned to the Wyckoff positions 2*b*, 4*e*, and 4*f* in the single crystal refinement due to the shortest Si–X distances, which is in accordance with lattice-energy calculations (see Supporting Information). In order to achieve charge neutrality, three positions are mixed occupied by isolated O- and F-atoms with an atomic ratio O/F = 1:1. The approximate ratio of the heavier elements (Ln/Si) was determined by energy dispersive X-ray microanalysis and confirms the X-ray structure refinement.

The layer silicates $Li_{14}Ln_5[Si_{11}N_{19}O_5]O_2F_2$ with Ln = Ce, Nd consist of *dreier* and *sechser* rings of corner sharing $[SiN_4]$ tetrahedra with an unprecedented topology (cf. Figure 1).[32]

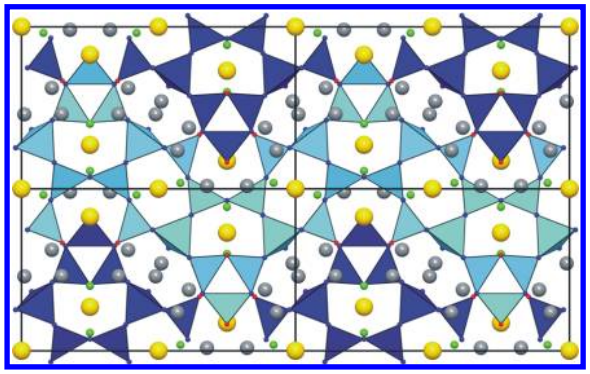

Figure 1. Crystal structure of $Li_{14}Nd_5[Si_{11}N_{19}O_5]O_2F_2$ (Ln = Ce, Nd) viewed along [010]. $[SiX_4]$ tetrahedra (X = N, O) are depicted in blue, with one layer motif highlighted in light blue. (N^{3-} dark blue, O^{2-} red, Ln^{3+} yellow, mixed $O/F^{-1.5}$-positions green, and Li^+ gray).

The layers are parallel to [101], and exhibit with κ = 11:24 an uncommonly high degree of condensation, which is usually 2:5 for layer (oxo)silicates. The high degree of condensation can be explained with the topology of the layers, as these have a relatively large layer thickness and the distance to the next layer is rather low. The Si–O distances vary from 1.677(13) to 1.705(8) Å for Ln = Ce and from 1.683(12) to 1.693(7) Å for Ln = Nd, respectively. The Si–N distances are slightly larger with 1.706(9) – 1.778(8) Å and 1.710(14) – 1.771(12) Å for Ln = Ce and Nd. These ranges are in agreement with the sum of the ionic radii (Si–O: 1.64 Å, Si–N: 1.69 Å)[33] and within the values of other oxonitridosilicates.[12,34]

There are three crystallographically independent Ln^{3+} sites which occupy the Wyckoff positions 2*a* (Ln1), 4*e* (Ln2), and 4*c* (Ln3). Ln1 is situated between the layers and exhibits a coordination sphere consisting of four O and three N in a distorted pentagonal bipyramidal arrangement. The other two Ln^{3+} sites are centered in the *sechser* rings of the layers and each is coordinated by eight electronegative atoms. The distances Ln–X (X = N, O, F) in these polyhedra range between 2.335(11) and 2.828(8) Å for Ln = Ce, and 2.320(9)–2.864(8) Å for Ln = Nd, respectively. The sum of the ionic radii corresponds well with the distances found in the different coordination spheres.[33] Furthermore, other well-investigated (oxo)nitridosilicates exhibit similar distance ranges.[27,35−37]

Four of the five crystallographically independent Li^+ sites in the crystal structure are situated between the layers in the resulting voids of the structure. These Li^+ sites build up double strands along the crystallographic *b*-axis (cf. Figure 2). The

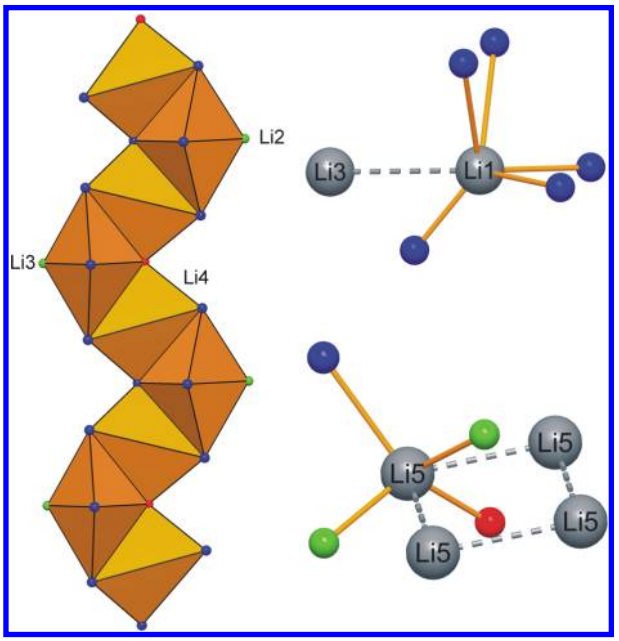

Figure 2. Coordination spheres of the Li^+ sites. Left: Polyhedral strand of alternating distorted tetrahedra and trigonal bipyramides of Li2–Li4. Right: coordination sphere of Li1 and Li5. Nitrogen blue, oxygen red, mixed occupied O/F green and lithium gray.

coordination spheres of these ions are alternatingly distorted tetrahedra (around Li4) and distorted trigonal bipyramides (around Li2 and Li3) made up from the electronegative atoms in the structure (Figure 2). The polyhedra are interconnected via common edges. Conjoined to Li3, which means to every fourth Li^+ site of a strand is an additional polyhedron centered around Li1 with a pyramidal coordination. In the structure, two strands are always positioned together, with one strand mirror-inverted and staggered to the other, building interlocked pairs (Figure 3). The distances in these polyhedra vary between 1.87(3) and 2.514(15) Å for Ln = Ce and 1.88(3) –2.494(15) Å for Ln = Nd, respectively, which is in accordance with the sum of the ionic radii and with other Li-containing compounds.[14,16,21,24,33,38] The fifth crystallographic Li^+ site (Li5) in the structure (Figure 2) is not interconnected with the Li-strands, but builds isolated $[Li_4X_{13}]^{28.5-}$ units (with X = N,O,F). The coordination of the Li^+ in this building unit is pyramidal.

The shortest interatomic Li–Li distances are situated within the strands and exhibit values in the range 2.44(3) – 2.62 Å (cf. Figure 3). In contrast, the lateral attached Li1 exhibit a slightly

dx.doi.org/10.1021/ja302255d | J. Am. Chem. Soc. 2012, 134, 10132–10137

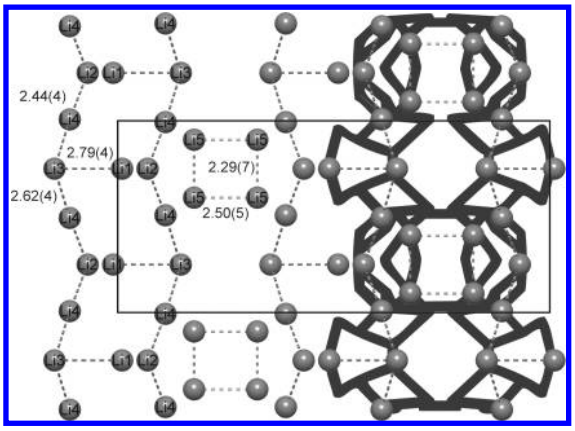

Figure 3. Li^+ positions in the crystal structure (view along [001]) with depicted shortest Li−Li distances in Å (standard deviations in parentheses) and calculated possible Li^+ pathways (dark gray) according to the voids in the structure.

higher distance to the neighboring Li (Li3) in the strands (2.86(4) Å for Ln = Ce, and 2.79(4) Å for Ln = Nd).

Structural Analysis of Possible Lithium Migration Pathways. An analysis concerning voids and migration pathways in the title compounds has been performed. In this context, the program package TOPOS has been employed.[39−41] Hereby, the voids in crystal structures are calculated with the help of Voronoi-Dirichlet polyhedra. The analysis of $Li_{14}Ln_5[Si_{11}N_{19}O_5]O_2F_2$ (Ln = Ce, Nd) on basis of the crystal structure refinement lead to possible 1D migration pathways along the crystallographic *b*-axis shown in Figure 3. A comparison of the shortest distance Li−Li with the pathways calculated due to the voids, which are suitable for lithium migration, shows that these do not coincide. The calculated pathways also include the seemingly isolated positions Li5. Anurova et al. calculated the voids of more than 2000 known compounds containing Li^+ ions with the program TOPOS and all compounds exhibiting infinite lithium pathways are either experimentally proven lithium ion conductors or are promising candidates for lithium ion conductors.[42] According to these calculations, anisotropic lithium ion conductivity is plausible with respect to the structural chemistry of the title compounds.

Electrical Conductivity Measurements. Figure 4 shows the Nyquist plot of the impedance spectrum acquired from the $Ti/Li_{14}Ln_5[Si_{11}N_{19}O_5]O_2F_2/Ti$ cell (the sample was kept at 300 °C for 20 h). One high frequency contribution (which can be fitted with an *RQ* equivalent circuit, *R* being the resistance and *Q* a constant phase element defined as $C = (R^{1-n}Q)^{1/n}$,

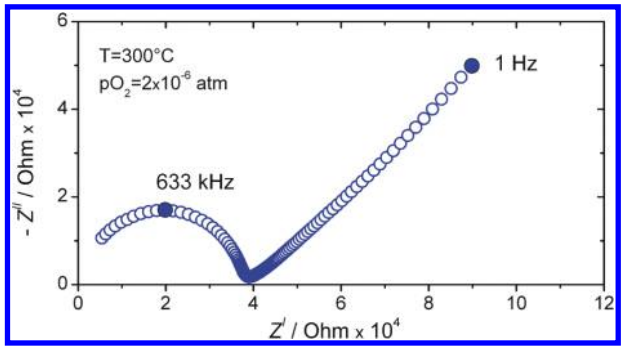

Figure 4. Impedance Nyquist plot of a spectrum collected from the $Ti/Li_{14}Ln_5[Si_{11}N_{19}O_5]O_2F_2/Ti$ cell.

where *C* is the capacitance and *n* an additional fitting parameter) followed by a Warburg behavior can be clearly recognized. The conductivity associated with the high frequency semicircle is on the order of 5×10^{-5} S/cm at 300 °C, while its capacitance value is ~6 pF ($\varepsilon_r \approx 80$). Notably, the appearance of a Warburg behavior in the presence of Ti electrodes indicates the occurrence of ionic diffusion. Impedance spectra were recorded during cooling every 20 K and upon a dwell time of 1 h at each step. Figure 5 illustrates

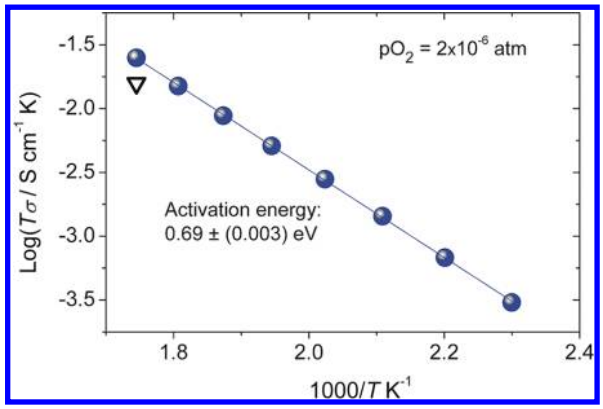

Figure 5. Arrhenius diagram obtained from the impedance spectroscopy measurements carried out with titanium electrodes.

the corresponding Arrhenius plot obtained after fitting the high frequency contribution: The activation energy is 0.69 eV. From these data, it is possible to extrapolate the electrical conductivity at room temperature, which is on the order of 1.7×10^{-10} S/cm. It is worth noting that additional tests were also performed with platinum electrodes and very similar values of conductivity as well as activation energy were obtained. The black triangle symbol in Figure 5 corresponds to a measurement performed at the end of all AC and DC measurements (see below). The sample exhibits only a minor degradation of the conduction properties.

DC polarization/depolarization measurements were also performed on the same $Ti/Li_{14}Ln_5[Si_{11}N_{19}O_5]O_2F_2/Ti$ cell. As shown in Figure 6(a), the change of the potential U upon the application of a DC current of 10 nA is not instantaneous, but rather exhibits the occurrence of an evident polarization process, which confirms the ionic character of the electrical conduction. If one compares the DC resistance at the plateau with the AC resistance values of the high frequency contribution of the impedance spectra [Figure 6(b)], then the ionic transference number (>0.99 at 300 °C) can be estimated.

In order to verify whether the ionic conductivity was indeed due to the Li ion migration, the second cell was prepared so as to block the electron transport and let lithium ions migrate: $LiAl/LiI/Li_{14}Ln_5[Si_{11}N_{19}O_5]O_2F_2/LiI/LiAl$.

The results of the polarization/depolarization measurement performed on the cell with electron-blocking elements are shown in Figure 7. Upon switching on a DC current of 10 nA, an instantaneous change of the potential U was recorded. Only a minor deviation from the ideal behavior was detected at the beginning of the polarization test. An analogous behavior characterizes the depolarization process when the current was turned off.

The resistance values obtained from the voltage plateau correspond to a conductivity on the order of 2.4×10^{-10} S/cm,

dx.doi.org/10.1021/ja302255d | J. Am. Chem. Soc. 2012, 134, 10132−10137

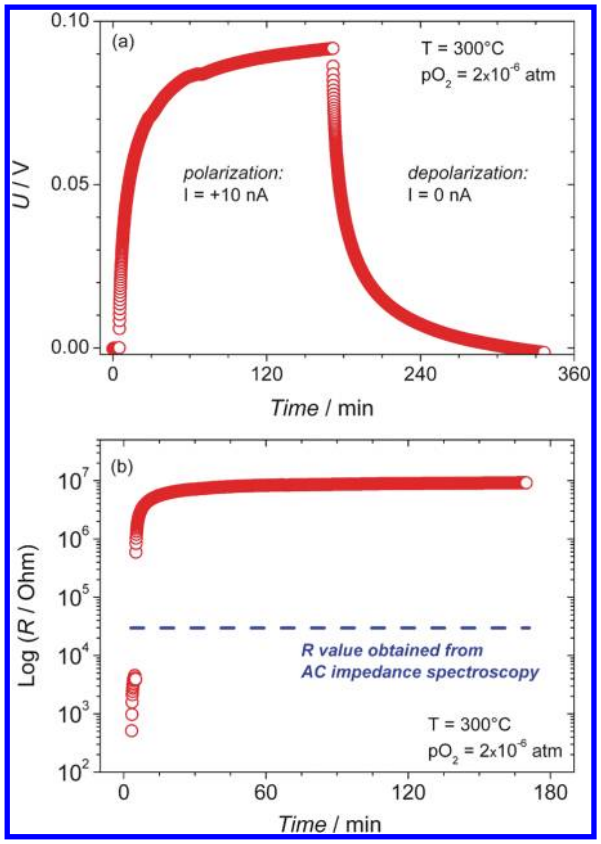

Figure 6. DC polarization/depolarization measurements: (a) polarization voltage as function of time for an applied current of 10 nA. (b) Resistance values obtained from (a); the AC resistance (cf. Figure 5) is shown for comparison.

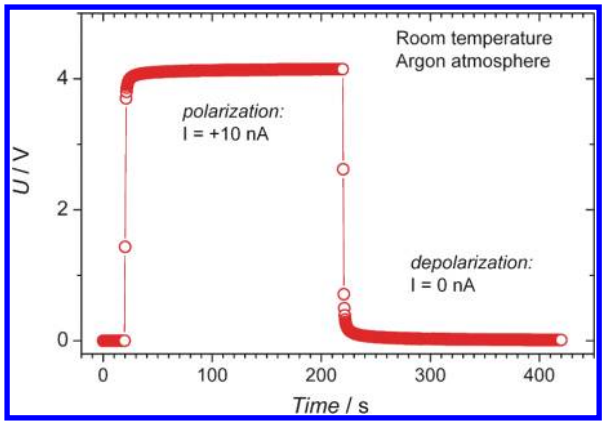

Figure 7. Time dependence of DC polarization and depolarization voltage for the LiAl/LiI/$Li_{14}Ln_5[Si_{11}N_{19}O_5]O_2F_2$/LiI/LiAl cell.

in very good agreement with the conductivity values extrapolated from the data of Figure 6.

AC impedance spectra were also acquired from this cell. In this case, two semicircles could be recognized. As the high frequency contribution exhibited a resistance that was ~500 times lower than the second one, one can safely assign it to the LiI elements. The second semicircle, whose conductivity was equal to ~6×10^{-10} S/cm could be ascribed to the $Li_{14}Ln_5[Si_{11}N_{19}O_5]O_2F_2$ layer.

Although such values of lithium ion conductivity are rather low compared with other solid-state electrolytes,[3] it is important to emphasize that the samples investigated here were simply cold pressed and not sintered. Therefore, one can expect the ionic conduction to improve upon the adjustment of the sintering conditions. More importantly, it is worth noting that the stoichiometry of $Li_{14}Ln_5[Si_{11}N_{19}O_5]O_2F_2$ has not been optimized yet as far as the ion transport properties are concerned. In the light of the unique structure of the phases considered here (the Li^+ sites create double strands along the crystallographic *b*-axis, see Figures 2 and 3), one can expect a significantly enhanced conductivity (within these strands) upon doping with aliovalent cations. In this context, it is important to recall that doping $LiSi_2N_3$ with Ca^{2+} resulted in an ionic conductivity enhancement up to 4 orders of magnitude, while the activation energy decreased from 0.69 eV (undoped) down to 0.22 eV.[43]

In summary, the high chemical (resistivity against air, moisture, and acids) and thermal (up to 900 °C measured) stability—characteristic for most (oxo)nitridosilicates[12]—of $Li_{14}Ln_5[Si_{11}N_{19}O_5]O_2F_2$ with Ln = Ce, Nd combined with the lithium ion conductivity makes this material interesting for future research.

CONCLUSIONS

In this contribution, we present the novel oxonitridosilicate $Li_{14}Nd_5[Si_{11}N_{19}O_5]O_2F_2$ and the isotypic Ce-containing phase. The compounds exhibit an unprecedented structure with a silicate substructure consisting of *dreier* and *sechser* rings of corner sharing tetraheda building layers. Structural analysis performed using the program TOPOS predicts lithium ion migration along the preferential crystallographic *b*-axis. Electrical conductivity measurements (DC as well as AC impedance spectroscopy) confirm the ionic character of the electrical transport (the ionic transference number is larger than 0.99 at 300 °C). The lithium ion conductivity is on the order of 5×10^{-5} S/cm at 300 °C with an activation energy of 0.69 eV.

These results indicate that these undoped (oxo)-nitridosilicates, a class of materials of which a number of different phases has already been structurally elucidated, represent a family of potential lithium ion conductors, whose defect chemistry needs however to be optimized (e.g., through aliovalent cation doping).

ASSOCIATED CONTENT

Supporting Information

Rietveld refinement of $Li_{14}Ln_5[Si_{11}N_{19}O_5]O_2F_2$ with Ln = Ce, Nd. Atomic coordinates, Wyckoff symbols, anisotropic displacement parameters, and selected distances for $Li_{14}Ln_5[Si_{11}N_{19}O_5]O_2F_2$ (Ln = Ce, Nd). Madelung part of lattice calculations to prove the electrostatic consistency of the compounds. This material is available free of charge via the Internet at http://pubs.acs.org.

AUTHOR INFORMATION

Corresponding Author

wolfgang.schnick@uni-muenchen.de

Notes

The authors declare no competing financial interest.

ACKNOWLEDGMENTS

The authors are indebted to the following people for conducting the physical measurements: Thomas Miller (single-crystal X-ray diffractometry and high temperature PXRD) and Christian Minke (X-ray microscopy), both at

LMU. We gratefully acknowledge financial support that was granted by the Fonds der Chemischen Industrie (FCI) and the Deutsche Forschungsgemeinschaft (DFG), project SCHN 377/14-1. Oliver Gerbig is thanked for his support during assembling the LiAl/LiI/$Li_{14}Ln_5[Si_{11}N_{19}O_5]O_2F_2$/LiI/LiAl cell.

REFERENCES

(1) Oudenhoven, J. F. M.; Baggetto, L.; Notten, P. H. L. *Adv. Energy Mater.* **2011**, *1*, 10−33.
(2) Whittingham, M. S. *Chem. Rev.* **2004**, *104*, 4271−4301.
(3) Park, M.; Zhang, X.; Chung, M.; Less, G. B.; Sastry, A. M. *J. Power Sources* **2010**, *195*, 7904−7929.
(4) Armand, M.; Tarascon, J.-M. *Nature* **2008**, *451*, 652−657.
(5) Kamaya, N.; Homma, K.; Yamakawa, Y.; Hirayama, M.; Kanno, R.; Yonemura, M.; Kamiyama, T.; Kato, Y.; Hama, S.; Kawamoto, K.; Mtsui, A. *Nat. Mater.* **2011**, *10*, 682−686.
(6) Masquelier, C. *Nat. Mater.* **2011**, *10*, 649−650.
(7) Robertson, A. D.; West, A. R.; Ritchie, A. G. *Solid State Ionics* **1997**, *104*, 1−11.
(8) Bruce, P. G.; West, A. R. *J. Solid State Chem.* **1982**, *44*, 354−365.
(9) Yashima, M.; Itoh, M.; Inaguma, Y.; Morii, Y. *J. Am. Chem. Soc.* **2005**, *127*, 3491−3495.
(10) Kanno, R.; Hata, T.; Kawamoto, Y.; Irie, M. *Solid State Ionics* **2000**, *130*, 97−104.
(11) Du, Y. A.; Holzwarth, N. A. W. *Phys. Rev. B* **2010**, *81*, 184106/1−184106/15.
(12) Zeuner, M.; Pagano, S.; Schnick, W. *Angew. Chem.* **2011**, *123*, 7898−7920; *Angew. Chem., Int. Ed.* **2011**, *50*, 7754−7775.
(13) Schnick, W. *Angew. Chem.* **1993**, *105*, 846−858; *Angew. Chem., Int. Ed. Engl.* **1993**, *33*, 806−818.
(14) Orth, M.; Schnick, W. *Z. Anorg. Allg. Chem.* **1999**, *625*, 1426−1428.
(15) Lang, J.; Charlot, J.-P. *Rev. Chim. Miner.* **1970**, *7*, 121−131.
(16) Pagano, S.; Zeuner, M.; Hug, S. *Eur. J. Inorg. Chem.* **2009**, 1579−1584.
(17) Yamane, H.; Kikkawa, S.; Koizumi, M. *Solid State Ionics* **1987**, *25*, 183−191.
(18) Juza, R.; Weber, H. H.; Meyer-Simon, E. *Z. Anorg. Allg. Chem.* **1953**, *273*, 48−64.
(19) Dadd, A. T.; Hubberstey, P. *J. Chem. Soc., Dalton Trans.* **1982**, 2175−2179.
(20) Hillebrecht, H.; Cruda, J.; Schröder, L.; Schnering, H. G. v. *Z. Kristallogr. Suppl.* **1993**, *6*, 80.
(21) Bhamra, M. S.; Fray, D. J. *J. Mater. Sci.* **1995**, *30*, 5381−5388.
(22) Pagano, S.; Lupart, S.; Zeuner, M.; Schnick, W. *Angew. Chem.* **2009**, *121*, 6453−6456; *Angew. Chem., Int. Ed. Engl.* **2009**, *48*, 6335−6338.
(23) Pagano, S.; Lupart, S.; Schmiechen, S.; Schnick, W. *Z. Anorg. Allg. Chem.* **2010**, *636*, 1907−1909.
(24) Lupart, S.; Pagano, S.; Oeckler, O.; Schnick, W. *Eur. J. Inorg. Chem.* **2011**, 2118−2123.
(25) Lupart, S.; Zeuner, M.; Pagano, S.; Schnick, W. *Eur. J. Inorg. Chem.* **2010**, 2636−2641.
(26) Lupart, S.; Schnick, W. *Z. Anorg. Allg. Chem.* **2011**, *638*, 94−97.
(27) Lupart, S.; Durach, D.; Schnick, W. *Z. Anorg. Allg. Chem.* **2011**, *637*, 1841−1844.
(28) Lange, H.; Wötting, G.; Winter, G. *Angew. Chem.* **1991**, *103*, 1606−1625; *Angew. Chem., Int. Ed. Engl.* **1991**, *30*, 1579−1597.
(29) Hofman-Bang, N. *Acta Chem. Scand.* **1957**, *11*, 581−582.
(30) Sheldrick, G. M. *Acta Crystallogr. A* **2008**, *64*, 112−122.
(31) Further details of the crystal structure investigation can be obtained from the Fachinformations-Zentrum Karlsruhe, 76344 Eggenstein-Leopoldshafen, Germany (fax: (+49)7247−808−666; e-mail: crysdata@fiz-karlsruhe.de) on quoting the depository numbers CSD-424264 for Ln = Ce, and CSD-424265 for Ln = Nd, the names of the authors and citation of the publication.
(32) The terms *dreier* and *sechser* rings were coined by Liebau and are derived from the German words "drei" (three) and "sechs" (six); however, for example a *dreier* ring is not a three-membered ring, but a six-membered ring comprising *three* tetrahedra centres.
(33) Shannon, R. D. *Acta Crystallogr., Sect. A: Cryst. Found. Crystallogr.* **1976**, *32*, 751−767.
(34) Schnick, W.; Huppertz, H. *Chem.—Eur. J.* **1997**, *3*, 679−683.
(35) Woike, M.; Jeitschko, W. *Inorg. Chem.* **1995**, *34*, 5105−5108.
(36) Huppertz, H.; Schnick, W. *Angew. Chem.* **1997**, *109*, 2765−2767; *Angew. Chem., Int. Ed.* **1997**, *36*, 2651−2652.
(37) Schmolke, C.; Bichler, D.; Johrendt, D.; Schnick, W. *Solid State Sci.* **2009**, *11*, 389−394.
(38) Zeuner, M.; Pagano, S.; Hug, S.; Pust, P.; Schmiechen, S.; Scheu, C.; Schnick, W. *Eur. J. Inorg. Chem.* **2010**, 4945−4951.
(39) Blatov, V. A. *Acta Crystallogr., Sect. A: Cryst. Found. Crystallogr.* **2000**, *56*, 178−188.
(40) Blatov, V. A.; Shevchenko, A. P.; Serezhkin, V. N. *J. Appl. Crystallogr.* **2000**, *32*, 377.
(41) Blatov, V. A. *IUCr Comp. Comm. Newsletter* **2006**, *7*, 4−38.
(42) Anurova, N. A.; Blatov, V. A.; Ilyushin, G. D.; Blatova, O. A.; Ivanov-Schitz, A. K.; Dem'yanets, L. N. *Solid State Ionics* **2008**, *179*, 2248−2254.
(43) Narimatsu, E.; Yamamoto, Y.; Takeda, T.; Nishimura, T.; Hirosaki, N. *J. Mater. Res.* **2011**, *26*, 1133−1142.